J. Biomedical Science and Engineering, 2013, 6, 61-70 **JBiSE**
http://dx.doi.org/10.4236/jbise.2013.612A008 Published Online December 2013 (http://www.scirp.org/journal/jbise/)

Modeling the effects of stretch-dependent surfactant secretion on lung recruitment during variable ventilation

Samir D. Amin[1], Arnab Majumdar[1], Phil Alkana[2], Allan J. Walkey[2], George T. O'Connor[2], Béla Suki[1*]

[1]Department of Biomedical Engineering, Boston University, Boston, USA
[2]School of Medicine, Boston University, Boston, USA
Email: [*]bsuki@bu.edu

Received 24 October 2013; revised 26 November 2013; accepted 15 December 2013

ABSTRACT

Variable ventilation (VV) is a novel strategy of ventilatory support that utilizes random variations in the delivered tidal volume (V_T) to improve lung function. Since the stretch pattern during VV has been shown to increase surfactant release both in animals and cell culture, we hypothesized that there were combinations of PEEP and V_T during VV that led to improved alveolar recruitment compared to conventional mechanical ventilation (CV). To test this hypothesis, we developed a computational model of stretch-induced surfactant release combined with abnormal alveolar mechanics of the injured lung under mechanical ventilation. We modeled the lung as a set of distinct acini with independent surfactant secretion and thus pressure-volume relationships. The rate of surfactant secretion was modulated by the stretch magnitude that an alveolus experienced per breath. Mechanical ventilation was simulated by delivering a prescribed V_T at each breath. The fractional V_T that each acinus received depended on its local compliance relative to the total system compliance. Regional variability in V_T thus developed through feedback between stretch and surfactant release and coupling of regional V_T to ventilator settings. The model allowed us to simulate patient-ventilator interactions over a wide range of PEEPs and V_Ts during CV and VV. Full recruitment was achieved through VV at a lower PEEP than required for CV. During VV, the acini were maintained under non-equilibrium steady-state conditions with breath-by-breath fluctuations of regional V_T. In CV, alveolar injury was prevented with high-PEEP-low-V_T or low-PEEP-high-V_T combinations. In contrast, one contiguous region of PEEP-V_T combinations allowed for full recruitment without overdistention during VV. We found that maintaining epithelial cell stretch above a critical threshold with either PEEP or V_T may help stabilize the injured lung. These results demonstrate the significance of patient-ventilator coupling through the influence of cellular stretch-induced surfactant release on the whole lung stability.

Keywords: Computational Modeling; Mechanical Ventilation; Variable Ventilation; Surfactant Secretion Dynamics

1. INTRODUCTION

Acute lung injury (ALI) and acute respiratory distress syndrome (ARDS) represent a continuum of lung injury that affects over 200,000 patients in the US yearly, with a 30% - 40% mortality rate [1]. The ALI and ARDS arise from either systemic insult (e.g., sepsis, pancreatitis) or local injury (e.g., pneumonia, aspiration injury) and manifest as acute inflammatory edema and diffuse alveolar damage. The inflammatory responses result in severely impaired lung function with reduced compliance and gas exchange, often culminating in respiratory failure and the need for mechanical ventilation. Currently, the only therapy that improves survival in ALI/ARDS is the ARDSNet ventilatory protocol, which decreases ventilator-associated lung injury (VALI) by avoiding alveolar overdistention [2].

In addition to alveolar overdistention injury, VALI can also be induced through the gradient of normal forces acting on epithelial cells during the reopening process of closed units [3,4]. These alveolar collapse-associated causes of VALI are attenuated by the addition of positive end expiratory pressure (PEEP), which is intended to recruit atelectatic lung, prevent alveolar surfactant depletion and end expiratory collapse. Unfortunately, the addi-

[*]Corresponding author.

tion of PEEP can lead to further overdistention and injury of healthy, high compliance alveolar units [5]. The success of mechanical ventilation depends on the right balance between overdistention and cyclic collapse-induced injury [6]. Although the ARDSNet strategy was a major advance in critical care, this method of mechanical ventilation did not completely eliminate VALI [7]. Thus, alternative mechanical ventilation strategies that can better balance overdistention and cyclic collapse have been sought.

Variable ventilation (VV) is a relatively novel strategy of ventilatory support that utilizes random variations in the delivered tidal volume (V_T) to improve lung function [Much]. Multiple pre-clinical models of acute lung injury have shown VV to be superior to conventional mechanical ventilation in inducing endogenous surfactant secretion [8,9], improving alveolar recruitment [10,11], and reducing cytokine [11,12] and histologic [13] evidence of VALI. Several mechanisms have been proposed to explain the benefit from adding variability to mechanical ventilation including variations along the nonlinear pressure-volume curve of the injured lung [14], time dependent closure and opening [11] and variable stretch-induced surfactant release [8,9].

Single large stretches have been shown to be a potent stimulus for surfactant release [15]. On the other hand, monotonous large amplitude cyclic stretch of epithelial cells in culture down-regulates surfactant release [8]. Thus, different stretch patterns delivered by a mechanical ventilation mode should have a significant impact on surfactant turnover which in turn determines lung compliance and hence patient outcome. To our knowledge, interactions among PEEP and V_T during mechanical ventilation, surfactant release and lung physiology have not been studied in a systematic way.

Combined with PEEP, VV has been shown to outperform CV in recruitment and reduction of epithelial injury in HCl-injured mice [12]. We thus hypothesized that there were combinations of PEEP and V_T during VV that led to improved alveolar recruitment through stretch-induced surfactant release compared to conventional mechanical ventilation (CV). To test this hypothesis, we have developed a computational model of stretch-induced surfactant production and release combined with abnormal alveolar mechanics of the injured lung during mechanical ventilation. Using this model, we compared alveolar recruitment-derecruitment behavior over a wide range of PEEP and V_T during both VV and CV.

2. METHODS

We model the lung as a parallel arrangement of N_A acinar units (**Figure 1(A)**), each with independent surfactant secretion and thus pressure-volume (*P-V*) relationship. Each acinar unit is assumed to consist of many alveoli which are not modeled separately. Within an acinar unit, surfactant secreted by type II epithelial cells accumulates onto the air-liquid interface to reduce surface tension and thus increase local alveolar compliance (**Figure 1(C)**). Epithelial cells secrete surfactant at a rate determined by the magnitude of stretch their unit experiences over a given breath (**Figure 1(B)**). Units that receive either more or less than average regional V_T also experience correspondingly more or less stretch; over time this will affect the amount of surfactant accumulated locally at the air-liquid interface and thus each unit consequently softens or stiffens.

The model simulates mechanical ventilation by delivering a prescribed V_T to the entire parallel set of acinar units each breath. The fractional tidal volume (V_{Ti}) that the *i*-th unit receives depends on its local compliance relative to the total compliance of the system (**Figure 1(D)**). Regional variability in V_T can thus develop through 1) the feedback between stretch and surfactant release, and 2) the coupling of regional V_T to mechanical ventilator settings. We can then compare this coupling behavior during simulated CV and VV of the lung model.

2.1. Modulation of Surfactant Release by Periodic Stretch

Alveolar tissue stretches to accommodate the variations in lung volume during ventilation. We define the magnitude of stretch ε in a unit over a given breath as the relative change in surface area at end-expiration A_{EE} to that at end-inspiration A_{EI}. Thus, ε approximately represents the biaxial strain the cells experience during tidal ventilation assuming that surface area of a single cell is much smaller than A_{EE}.

It is well documented that surfactant release increases with stretch amplitude up to moderate strains [15,16], while large stretch inhibits release [8,16]. It naturally follows that there must be some intermediate stretch level that produces a peak in surfactant release, although the exact relation has yet to be determined.

Thus, to incorporate in the model stretch-induced cellular surfactant release and inhibition (from excessive stretch) in a simple manner, we assume that the rate of surfactant release in a unit increases with stretch magnitude until ε surpasses a critical threshold ε^*, whereby surfactant release reduces with further stretch magnitude (**Figure 1(B)**). A piecewise linear relation is used for surfactant release rate φ as a function of ε:

$$\varphi = \begin{cases} \dfrac{\varepsilon}{\varepsilon^*} & \varepsilon \le \varepsilon^* \\ 2 - \dfrac{\varepsilon}{\varepsilon^*} & \varepsilon^* \le \varepsilon \le 2\varepsilon^* \\ 0 & \varepsilon > 2\varepsilon^* \end{cases} \quad (1)$$

Note that in the context of the model, the exact linear shape is not important; it's the existence of a peak that we aim to capture. Furthermore this curve only represents the stretch-dependent fraction of surfactant release, which is in addition to a baseline rate which we assume is constant throughout the simulation. This point is elaborated on in Section 4.2.

2.2. Dynamics of Surfactant Secretion and Degradation

We propose a simple first order dynamics description of surfactant secretion (**Figure 1(C)**). Stretch ε induces the release of surfactant. At each breath n, a small amount of surfactant is released from the cells onto the alveolar air-liquid interface. Interfacial surfactant (S) is simultaneously removed through degradation, uptake or other processes at a rate λ so that S at breath $n+1$ is given by:

$$S_{n+1} = (1-\lambda)S_n + \varphi_n \tag{2}$$

2.3. Sigmoidal Pressure-Volume Relation

The volume V of each acinar unit obeys a sigmoid relation with transpulmonary pressure P:

$$V = \frac{V_{\max}}{1+e^{-\kappa(P-G)}} \tag{3}$$

The parameter κ corresponds to the compliance of the curve, $V_{\max}$ is the volume at total lung capacity (TLC) and G is the inflection point. The P-V curve of each acinus, which we assume is proportional to the entire volume of the unit, is modulated breath-by-breath by the available interfacial surfactant S_n as

$$G_n = G_0 e^{-\frac{S_n}{S_0}} \tag{4}$$

where S_0 is a scaling parameter, and G_0 corresponds to the inflection point of **Eq.3** arising solely from the equilibrium amount of stretch-independent surfactant release. Thus, an increase in interfacial surfactant shifts the inflection point to the left resulting in a higher volume for a given pressure (**Figure 1(D)**). This form presented by [17] was chosen as it captures lung P-V curves under a variety of conditions, and is further discussed in Section 4.5.2.

2.4. Simulation of Mechanical Ventilation

Ventilation of the model is calculated using a prescribed PEEP and V_T as follows. We assume that all acinar pressures P_i reach equilibrium both at end expiration (EE) and end inspiration (EI), and thus tissue and surface film viscoelasticity is immaterial. Thus, at end expiration, the pressure in each unit is equal to the prescribed PEEP

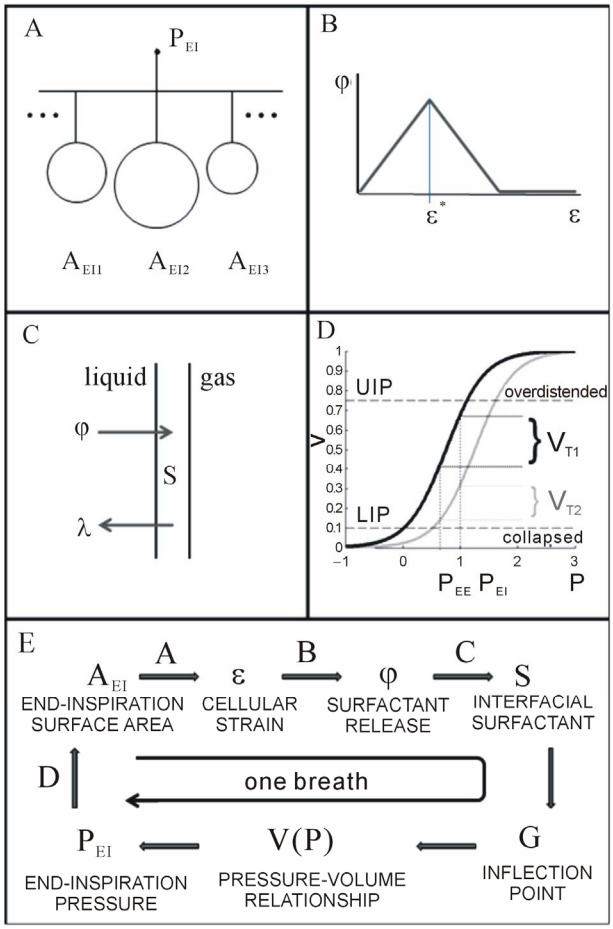

Figure 1. Total Surfactant Release and Regional Tidal Volume is Modulated by Periodic Stretch. (A) The lung is divided into parallel alveolar units each defining an acinus, and ventilated with a given tidal volume (V_T). Individual tidal volumes, and thus strains, vary with regional compliances. At end-inspiration with airway pressure P_{EI} each unit can have a different alveolar surface area A_{EI}. (B) Rate of surfactant secretion φ as a function of stretch amplitude ε of a single unit. (C) Schematic of the accumulation of surfactant (S) on the gas-liquid interface. Surfactant is also removed from the interface at a rate. (D) Sigmoid pressure-volume (P-V) relation of a single alveolar unit is shifted to the left with increasing interfacial surfactant (S). U_{IP} and L_{IP} denote the upper and lower inflection point, respectively. (E) Strains from previous breaths modulate surfactant levels which alter the P-V relationship of individual units and thus the strains for the next breath, resulting in a closed feedback loop. See text for further explanation.

with total lung volume V_{EE}. At the end of inspiration, the total lung volume V_{EI} increases above V_{EE} by the prescribed tidal volume V_T which is distributed among the acinar units labeled with i according to the stiffness of their individual pressure-volume P_i-V_i curve. Thus,

$$V_{EE} = \sum_i V_i\left(P = \text{PEEP}\right) \tag{5a}$$

$$V_{TARGET} = V_{EE} + V_T \tag{5b}$$

$$V_{EI} = \sum_i V_i \left(P = P_{EI} \right) \quad (5c)$$

where we replaced P_i with P both at end-inspiration and end-expiration. Once V_{EE} is determined from the previous breath according to **Eq.5a**, the target end-inspiratory volume V_{TARGET} is computed from **Eq.5b**. To ensure that total lung volume is equal to V_{EI} at end inspiration, P is increased by a small amount, the corresponding V_i of each unit is computed using **Eq.3**, and the sum on the right hand side of **Eq.5c** is determined. This process is iterated until the sum of the volumes V_i equals V_{TARGET}. The final value of P defines P_{EI} of the model, and is calculated with a maximum error tolerance of 0.01%. The surface areas A_{EE} and A_{EI} of each unit are then calculated from their respective volumes assuming sphericalacini. Note that regardless of the particular shape of each acinus, the area will scale with volume raised to the 2/3 power. The value of ε is computed from A_{EE} and A_{EI} as described above which is then used to determine surfactant secretion φ (**Eq.1**). Next, the amount of surfactant secreted over the current breath is determined by solving **Eqs.1** and **2**. Finally, S is substituted into **Eq.4** to determine all regional P-V curves for the next breath.

We simulate ventilation in discrete, breath by breath steps. Tidal volume $V_T = V_{T0}$ is fixed for each breath during CV simulations. For VV, V_T is uniformly distributed within 10% above and below V_{T0}. We set functional residual capacity (FRC) defined as V_{EE} in the absence of PEEP, TLC, and minute ventilation (MV) according to values for a standard adult male. Parameter values, found in **Table 1**, were scaled such that the FRC, TLC and MV correspond to those in the healthy human adult lung.

2.5. Introduction of Injury

2.5.1. Heterogeneity in Intracellular Surfactant Release

Starting at breath $n = N_{INJ}$, the efficiency of intracellular surfactant secretion φ is disrupted. This is implemented by multiplying $\varphi(n \geq N_{INJ})$ for each unit by a factor $(1 + \eta_i)$, where η_i is a random variable between −0.05 and 0.05. Note that η_i is selected once at N_{INJ}, and then each η_i is held constant over time for the duration of the simulation.

2.5.2. Heterogeneity in Regional Stiffness

An identical procedure was applied to varying acinar regional stiffness κ as with surfactant release described above.

Table 1. Parameter values.

Param	Value	Param	Value	Param	Value	Param	Value
N_A	1024	TLC	6.0 L	T	4 s	L	4E-3
FRC	2.5 L	MV	7.5 L/min	ε	0.13	G_0	1
V_T	0.5 L	V_{MAX}	TLC/NA	κ	2.97	S_0	1.72

3. RESULTS

We present two major results. First, our four unit simulation results in **Figure 2** demonstrate how PEEP can both increase long-term recruitment and also delay the eventual collapse of unrecoverable units in CV. In combination with VV, however, this delay can be made much

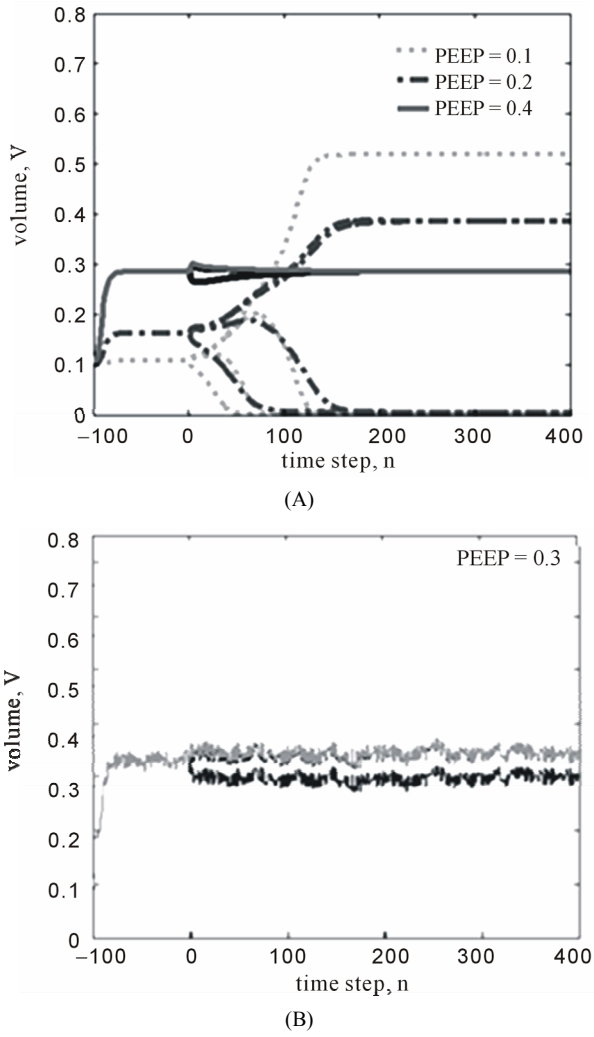

Figure 2. Four unit simulations. (A) End-inspiratory volumes V_{EI} stabilized by the application of PEEP during Conventional Ventilation. Dotted, dashed-dotted and solid lines correspond to PEEP = 0.1, 0.2 and 0.4, respectively. The four curves with each line type correspond to the four compartments. (B) Variable ventilation results in the lung reaching steady equilibrium, reducing the extent of alveolar collapse as compared to conventional ventilation. For clarity, here only the traces of the 4 units corresponding to PEEP = 0.3 are shown where all four units remain open. Notice that 3 units follow essentially the same pattern while the fourth is kept open at a slightly lower V_{EI}. This is the same unit that collapsed during CV at PEEP < 0.4.

longer as injured units appear to remain at non-equilibrium, fluctuating volumes. Second, during ventilation in the presence of heterogeneous surfactant release or tissue stiffness, we find that VV can maintain higher recruitment while avoiding overdistention for a wider range of PEEP and mean V_T values, partly through the mechanism described above.

3.1. Four Unit Simulations

We first simulated CV or VV of a lung model including only four units, tracing individual V_{EI} over time in **Figure 2** for PEEP values ranging from 0 to 0.4 (in arbitrary units). The simulations include an initial transient region between $n = -100$ and 0, where either CV or VV was applied in the absence of any injury. At $n = 0$, heterogeneity in intracellular surfactant release was introduced as described in the Methods, while CV or VV was continued for another 400 breaths. The injury was identical in the two cases.

For CV at PEEP = 0.1, three units collapsed following injury. Increasing PEEP to 0.2, there was a reduction to only 2 collapsed units and also an increased transient time for the second compartment to collapse. A full recruitment of all 4 units was still not achieved at PEEP = 0.3, and was qualitatively similar to the PEEP = 0.2 condition (not shown). With PEEP = 0.4, all 4 units are stretched beyond ε^*, and thus we observe stable behavior with full recruitment. In contrast to CV, full recruitment was achieved through the use of VV at the lower PEEP of 0.3. Notice that during VV, the acinar compartments were maintained under non-equilibrium steady-state conditions with breath-by-breath fluctuations of V_{EI}. Thus, the variability in delivered tidal volumes prevented the quick collapse of all injured acini.

3.2. Optimization of PEEP and V_T for Maximal Recruitment with Minimal Overdistention

We next simulated mechanical ventilation with a 1024 unit model as described in the Methods. Again, we tracked V_{EI} of each individual unit after introduction of injury at breath $n = 0$. However, we analyze two types of injury—heterogeneity in surfactant release and in acinar stiffness, for 20 values of PEEP and 30 values of V_T utilizing CV and VV. At the end of the simulation, the fraction of collapsed and overdistended units were determined and plotted as a function of PEEP and V_T.

Figure 3 presents the results for CV with heterogeneous injury to surfactant release. On the left panel, we see alveolar collapse with PEEP < 0.5 and $V_T < 0.5$. The extent of collapse gradually decreases with increasing V_T. On the other hand, there appears to be a distinct threshold around PEEP = 0.4 where collapse is completely avoided regardless of V_T. Overdistention defined as

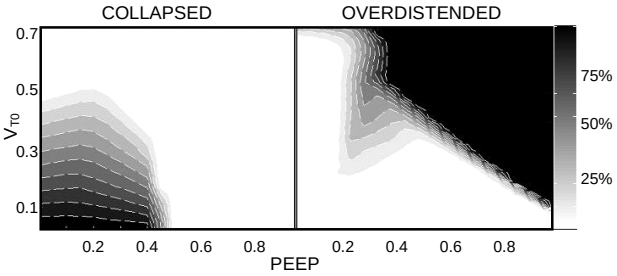

Figure 3. Alveolar collapse and overdistention in the presence of surfactant heterogeneity during conventional ventilation. Contour plots describe the fraction of the lung in the specified category when ventilating with a given PEEP and V_T. Left: Fraction of collapsed alveoli reduces gradually with increasing V_T and sharply with PEEP. Right: Fraction of overdistended alveoli increases with PEEP at high tidal volumes.

$V_{EI} = V_{EE} + V_T$ reaching 75% of maximum alveolar volume showed an opposing trend, where the highest V_T which avoids overdistention decreases approximately linearly with increasing PEEP. Simultaneous collapse and overdistention can be observed at midrange values of PEEP and V_T.

Additional simulations allowed us to compare and contrast the results for applying VV or CV for heterogeneous surfactant release as well as heterogeneous acinar stiffness (**Figure 4**). For a disruption of normal homogeneous surfactant release under CV (top left panel), alveolar collapse occurs at low-PEEP-low-V_T settings, while overdistention occurs for high-PEEP-high-V_T settings resulting in two relatively small disjoint regions (blue) whereby alveolar injury is prevented. When VV is applied (top right panel), one contiguous region of PEEP and V_T allows for full recruitment without overdistention. Overall, the possible combinations of PEEP and V_T during VV are much greater than during CV. For the heterogeneous acinar stiffness case under CV (bottom left panel), again alveolar collapse occurs at low-PEEP-low-V_T settings, while overdistention occurs for high-PEEP-high-V_T settings. However, in this case a contiguous band of good PEEP-V_T settings exist. When VV is applied (right panel), the size of this region is significantly larger.

4. DISCUSSION

In this study, we developed a model that incorporates stretch-induced surfactant release into the regional pressure-volume curve of a parallel set of acinar units exposed to various ventilator settings. To our knowledge, this is the first attempt to couple surfactant metabolism with stretch and regional lung mechanics. The model allows us to simulate patient-ventilator interactions over a wide range of PEEPs and V_Ts. The primary finding of the study is that the particular ventilator settings have a critical role in surfactant distribution, regional lung compliance and hence predicted ventilation outcome.

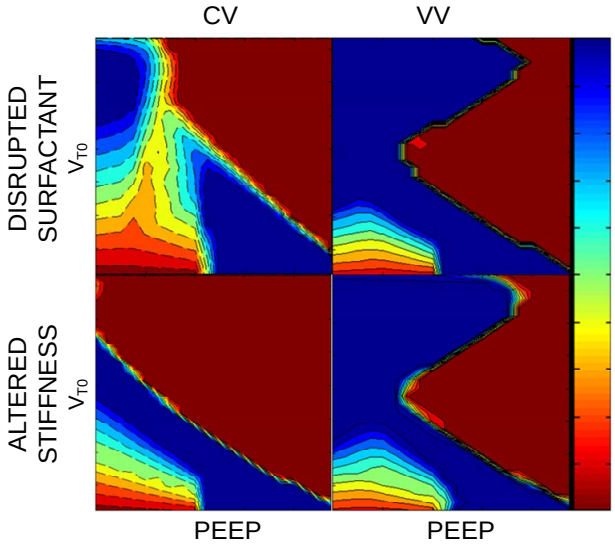

Figure 4. Comparison of best PEEP-V_T settings for CV vs. VV for two different pathologies. Contour plots describe the fraction of the lung which are neither collapsed nor overdistended when ventilating with a given PEEP and V_T for CV and VV. For instance, the top left panel shows the superimposed view of **Figures 3(A)** and **(B)**, presenting the PEEP and V_T settings which resulted in the best outcomes (number of units recruited but not overdistended) in blue and injury due to collapse or overdistention marked by red. Top left: Heterogeneous surfactant release under CV. Top right: Heterogeneous surfactant release under VV. Bottom left: Heterogeneous alveolar stiffness under CV. Bottom right: Heterogeneous alveolar stiffness under VV.

Specifically, VV provides a much wider range of possible ventilator settings that result in maximum lung recruitment and minimal overdistention when compared to CV.

4.1. Optimal PEEP-V_T Values for CV and VV

In this model, alveolar collapse is prevented by stretching the acinar units above ε^*. This can be accomplished through either large tidal stretches alone, by providing a sufficiently high PEEP such that $\varepsilon > \varepsilon^*$ at end expiration, or by a combination of both ventilator settings. This is reflected in the lower left-hand corner of each panel in **Figure 4**: low PEEP and small V_T leads to collapse whereas large V_T values provide adequate stretch and surfactant release. With increasing PEEP, a lower V_T is sufficient to produce the necessary stretch. At around PEEP = 0.4, the end-expiratory pressure alone is sufficient to maintain alveolar recruitment. Naturally, there is an inverse relationship between the V_T and PEEP required to reach the absolute volume beyond which overdistention of the alveoli occurs. The reason for this is that PEEP effectively increases V_{EE}. These characteristics are common to each simulation case.

The difference between VV and CV are illustrated in the presence of heterogeneous surfactant release in the top panels of **Figure 4**. As some acinar units collapse, their volume is diverted into the remaining units triggering simultaneous collapse and overdistention as seen in the top left panel of **Figure 4**. However, we observe that VV allows for full recruitment at a lower V_T than CV. In fact, the overlapping region of collapse and overdistention is completely removed. Overall, a larger range of PEEP and V_T can provide optimal acinar recruitment (area of the blue regions) in VV than for CV.

We also note here a qualitative difference between the results for the two injury cases during CV. In the presence of heterogeneous stiffness, we no longer observe an area of simultaneous collapse and overdistention. The model also predicts a larger area of overdistention, and low-PEEP-high-V_T settings no longer produce a positive outcome (defined as full recruitment). In contrast, the acceptable combinations of PEEP and V_T during VV seem to be insensitive to the simulated injuries. Additional sensitivity analysis, in which model parameters were varied between 50% and 200% of their baseline values, indicated that the advantage of VV over CV is robust and does not depend on particular model settings.

In both cases of injury during VV, there exists an unexpected region at intermediate PEEPs where increasing tidal volume first causes and then prevents overdistention. We note that these PEEP-V_T combinations are well above physiologic values, and discuss this further in the section on model limitations.

4.2. Stability of the Alveolus through Stretch-Surfactant Relation

The shape of the stretch-surfactant relationship (**Figure 1(B)**), in particular its peak, has two consequences on model behavior. First, there appears to be an optimal stretch magnitude for surfactant secretion, and thus reduction of mechanical injury induced by ventilation. The second, seemingly counterintuitive, consequence is that optimal lung function actually requires the majority of the lung to be stretched beyond this threshold. Consider an alveolus ventilated at or below the stretch threshold ε^*. A minor reduction in stretch attenuates surfactant production, increasing stiffness which in turn further reduces stretch, eventually leading to full collapse. This is in agreement with recent data that ventilating normal mice at a PEEP of 3 cm H_2O for 30 min, a reduction in V_T from 8 to 6 ml/kg significantly reduced the level of surfactant protein B, a key component of surfactant that contributes to normal surface tension [18]. In contrast, in the regime above the stretch threshold, reduced/increased alveolar stretch increases/reduces surfactant production, and thus deviations from the initial stretch magnitude are countered by the stretch modulated surfactant secretion.

In other words, an inverse relation between stretch and surfactant secretion beyond the critical value ε^*, in combination with the nonlinear pressure-volume relationship, guarantees the stability of acinar units.

4.3. Coupling of Local Surfactant Secretion and Compliance to Regional Ventilation

Next, we consider several connected acinar units ventilated at a fixed global tidal volume such that the alveolar stretch magnitudes are beyond ε^*. If one alveolus is injured and thus stretched below the threshold, it would tend to collapse according to the mechanism described in Section 4.2, diverting its tidal volume into the remaining normal alveoli. This extra volume causes the normal alveoli to be stretched further above the threshold, reducing their surfactant thus increasing their stiffness. This redirects flow back into the injured unit, increasing its surfactant production possibly preventing collapse. This protective mechanism no longer holds, however, when the entirety of units are also stretched below the threshold. After a large fraction of the units collapse, the diverted tidal volume is forced into the small remaining open fraction of the units resulting in their overdistention. Consequently, a heterogeneous distribution of severe injury through surfactant interference or local trauma can result in neighboring regions of collapsed and overdistended acinar units. Images of subpleural alveoli of normal and ventilator-injured lungs are consistent with this notion (10). Thus, maintaining above-threshold stretch with either PEEP or tidal volume may help stabilize the injured lung.

4.4. Non-Equilibrium Steady State during Variable Ventilation

Through the proposed mechanisms, progressive alveolar collapse and ventilation redistribution occurred due to the instability of the system when stretch is below ε^*. During CV, the final outcome (e.g. whether an acinus collapses) was a function of the stretch magnitude of each acinus relative to the threshold. The time scale of collapse depended primarily on surfactant dynamics (φ and λ) and tidal volume, and in many cases a long transient period preceded equilibrium. During VV, the cycle-by-cycle variations of regional tidal volumes disrupted the stretch-surfactant coupling, prolonging this transient period indefinitely. Indeed, such dynamic equilibrium has been found experimentally in mice during ventilation with VV [19]. In our model, this steady state maintains on average a larger number of recruited acinar units than CV. We can speculate that in real patients, if such steady state exists, it may allow time for the injury to heal and thus faster return to normal function upon release from the ventilator. We also note that experimentally it was found that VV stimulates surfactant release as well as production [20]. Our simulations are consistent with this since on average a higher lung volume in the model is due to more surfactant. Thus, the non-equilibrium steady state seen in the model offers a mechanistic explanation for such experimental findings.

4.5. Model Limitations

Several assumptions in our model were implemented to simplify the dynamics and study regional surfactant metabolism coupled with regional alveolar stretch. Additionally, several important phenomena have also been neglected. These are discussed next.

4.5.1. Modeling Stretch-Induced Surfactant Release

Little is known about the stretch-induced dynamics of surfactant release and production in vivo. In vitro studies suggest that increasing the amplitude of a single biaxial stretch applied to cells in culture, increases the amount of surfactant released in a quasi-exponentially increasing manner while the time course of the release showed an asymptotic approach to a constant [15]. During cyclic stretch; however, large amplitudes down-regulated surfactant release [8]. The shape of the surfactant release-stretch curve in our model (**Figure 1(B)**) incorporated these observations. As described in Section 4.2, it is the slope of the stretch-surfactant curve below and above the peak that drives the stability of the overall system. In light of this, our choice of a linear relation as opposed to another would not qualitatively affect our results. This feature of the model together with how surfactant affects the pressure-volume curve (**Figure 1(D)**) led to the prediction of reversal of overdistention with unphysiologically large V_T values superimposed on medium PEEP levels. Nevertheless, VV still outperformed CV even if we did not include this region in the comparison.

4.5.2. Pressure-Volume Relation

We selected the empirical pressure-volume relation presented by [17] as it is able to capture the convex *P-V* relation at low volumes resulting from recruitment and the plateau at high pressures due to tissue stiffening. Our implicit assumption is that the *P-V* relation on the scale of individual acinar units is similar to that of the whole lung. In this manner, we are able to parameterize individual acinar units based on published values corresponding to whole lung data [17]. The disadvantage of an empirical curve is that it does not account for the contribution of tissue and surface forces separately.

Although the relation presented by Bachofen and Wilson [21] and subsequent modifications [22,23] explicitly includes the micromechanical response of fiber stretch and surface tension within individual acini, it is unsuitable to our needs as its applicability is limited be-

tween 40% and 80% of TLC, whereas our model necessarily contains acini outside of this range. The model presented by Denny and Shroter [24] contain surface and tissue forces similar to that of [21] at the level of individual acini, showing a sigmoidal relation qualitatively similar to [17] for the full range of volumes, but lacks an analytic *P-V* relation. We note that similar to the stretch-surfactant relation, the exact *P-V* relation does not quailtatively affect our results, but rather the second derivative of this curve (how stiffness varies with volume). Any sufficiently similar *P-V* curve would deliver similar results.

4.5.3. Parameter Selection

The exact values of many of our model parameters are difficult to quantify *in vivo*, and thus remain unknown. For instance, φ_{max} corresponds to the peak surfactant release rate per cell at a given stretch amplitude and frequency, while λ is the collective rate of several processes of surfactant depletion (re-uptake, enzymatic reuptake, de-activation, etc.). The exact shape of the φ versus ε relation is also unknown, and the effect of surfactant on the static *P-V* relationship of a single alveolus was only estimated as shifting the curve along the pressure-axis. To justify our parameter selection, we note that changing φ_{max} in our model amounts to multiplying φ by a constant proportionality factor for all units, and would not change the overall system's qualitative behavior. The degradation parameter λ effectively "smoothens out" the changes in surfactant from each breath: $\lambda = 1$ corresponds to immediate degradation of surfactant after each breath. Thus, adjusting λ affects the time course of collapse which is not systematically analyzed in this study, and does not alter the end result of the number of stable and collapsed acini. For the normal uninjured lung, we chose the values of φ_{max}, λ, G_0, and ε^* to correspond to a lung with FRC = 2.5 L and TLC = 6 L while ventilated with V_T = 0.5 L and PEEP = 0.

4.5.4. Breath-by-Breath Dynamics

Assuming full equilibrium of pressures both at end-expiration and end-inspiration neglected the presence intra-breath dynamics and discounted the effects of tissue and surface film viscoelasticity. As a result, the model is unable to reproduce hyperinflation, and the time dependence of the opening and closing processes has been neglected [25] that would likely further complicate the process of gradual collapse in the model. The surface area-surface tension loop depends on the constituents of the surfactant at the air-liquid interface and exhibits hysteresis during a breath cycle in overinflated but otherwise normal regions [26] which is not taken into account.

4.5.5. Parallel Compartment Model

Another simplification was that we modeled a parallel set of units; hence, any effects due to airway structure are absent. One important aspect of this may be that repeated airway opening and closing can produce shear and/or normal stresses [27] that would amplify epithelial injury. A further limitation is that due to the previous assumption of pressure equilibrium, applying a different pathway resistance for each parallel compartment would not introduce heterogeneous regional flow delivery and pressure fluctuations [28]. Additionally, inter-regional airflows causing heterogeneous emptying of the lung are not possible in our model.

4.5.6. Independent Lung Regions

In the current model, the coupling between regions is attributed to the redirection of tidal volume from stiffer to softer compartments in the presence of a fixed total tidal volume. The effects of fluid accumulation and the corresponding effects of gravity were not taken into account. Both of these phenomena have been shown to play a role in VALI (8) and future extensions of the model should explicitly incorporate them. Additionally, mechanical coupling through parenchymal interactions likely promotes regional interdependence.

4.5.7. Limited Injury Mechanisms

Finally, our models of lung injury at the alveolar and cellular levels are non-specific. For example, fluid leakage from the vasculature alters the composition and hence the surface-tension surface area relation of the surfactant [26]. Fluid accumulation in the alveoli changes the shape of the local *P-V* curve with a significant decrease in compliance [29]. These mechanisms of lung injuries should be explored since it is possible that the best PEEP-V_T combination is injury specific. For instance, atelectatic opening and closing may cause more lung injury than sustained collapse, as could high strain magnitudes without overdistention leading cell membrane rupture [30].

Despite the limitations discussed above, the novel features of the model allowed us to explore patient-ventilator coupling and optimization of best PEEP-V_T combination in the presence of collapse and overdistention injury. The main result was that the coupling between surfactant secretion and regional lung mechanics during ventilation has a significant impact on the outcome of patient ventilation. While this was possible only using an appropriate computational model due to the difficulties associated with the breath-by-breath experimental assessment of surfactant pool and regional lung mechanics, the long-term predictions of the model could be tested in clinical settings.

5. CONCLUSION

It is now well-acknowledged that protecting epithelial

cells from injury is the most important goal of any ventilation strategy. The model developed in this study demonstrates the significance of the cellular stretch-induced surfactant release relationship with respect to the whole lung stability. Maintaining epithelial cell stretch above a critical threshold with either PEEP or V_T may help stabilize the injured lung. Moreover, the injured lung can see additional benefit from breath-by-breath variation of tidal volumes which maintains the lung periphery open under a dynamic equilibrium with a better outcome than the corresponding conventional ventilation strategy. Thus, irrespective of the particular model used in this study, our results point to the clinical significance of ventilator-patient coupling.

6. ACKNOWLEDGEMENTS

Funded by HL-098976, HL-111745, DoD W81XWH-08-1-0148 and the Coulter Foundation.

REFERENCES

[1] Rubenfeld, G.D., Caldwell, E., Peabody, E., Weaver, J., Martin, D.P., Neff, M., Stern, E.J. and Hudson, L.D. (2005) Incidence and outcomes of acute lung injury. *The New England Journal of Medicine*, **353**, 1685-1693. http://dx.doi.org/10.1056/NEJMoa050333

[2] The Acute Respiratory Distress Syndrome Network (2000) Ventilation with lower tidal volumes as compared with traditional tidal volumes for acute lung injury and the acute respiratory distress syndrome. *The New England Journal of Medicine*, **342**, 1301-1308. http://dx.doi.org/10.1056/NEJM200005043421801

[3] Bilek, A.M., Dee, K.C. and Gaver 3rd., D.P. (2003) Mechanisms of surface-tension-induced epithelial cell damage in a model of pulmonary airway reopening. *Journal of Applied Physiology*, **94**, 770-783.

[4] Kay, S.S., Bilek, A.M., Dee, K.C. and Gaver 3rd., D.P. (2004) Pressure gradient, not exposure duration, determines the extent of epithelial cell damage in a model of pulmonary airway reopening. *Journal of Applied Physiology*, **97**, 269-276. http://dx.doi.org/10.1152/japplphysiol.01288.2003

[5] Puybasset, L., Gusman, P., Muller, J.C., Cluzel, P., Coriat, P. and Rouby, J.J. (2000) Regional distribution of gas and tissue in acute respiratory distress syndrome. III. Consequences for the effects of positive end-expiratory pressure. CT Scan ARDS Study Group. Adult Respiratory Distress Syndrome. *Intensive Care Medicine*, **26**, 1215-1227. http://dx.doi.org/10.1007/s001340051340

[6] Rouby, J.J. and Brochard, L. (2007) Tidal recruitment and overinflation in acute respiratory distress syndrome: Yin and yang. *American Journal of Respiratory and Critical Care Medicine*, **175**, 104-106. http://dx.doi.org/10.1164/rccm.200610-1564ED

[7] Terragni, P.P., Rosboch, G., Tealdi, A., Corno, E., Menaldo E, Davini, O., Gandini, G., Herrmann, P., Mascia, L., Quintel, M., Slutsky, A.S., Gattinoni, L. and Ranieri, V.M. (2007) Tidal hyperinflation during low tidal volume ventilation in acute respiratory distress syndrome. *American Journal of Respiratory and Critical Care Medicine*, **175**, 160-166. http://dx.doi.org/10.1164/rccm.200607-915OC

[8] Arold, S.P., Bartolak-Suki, E. and Suki, B. (2009) Variable stretch pattern enhances surfactant secretion in alveolar type II cells in culture. *American Journal of Physiology*: *Lung Cellular and Molecular Physiology*, **296**, L574-L581. http://dx.doi.org/10.1152/ajplung.90454.2008

[9] Arold, S.P., Suki, B., Alencar, A.M., Lutchen, K.R. and Ingenito, E.P. (2003) Variable ventilation induces endogenous surfactant release in normal guinea pigs. *American Journal of Physiology*: *Lung Cellular and Molecular Physiology*, **285**, L370-L375.

[10] Arold, S.P., Mora, R., Lutchen, K.R., Ingenito, E.P. and Suki, B. (2002) Variable tidal volume ventilation improves lung mechanics and gas exchange in a rodent model of acute lung injury. *American Journal of Respiratory and Critical Care Medicine*, **165**, 366-371. http://dx.doi.org/10.1164/ajrccm.165.3.2010155

[11] Bellardine, C.L., Hoffman, A.M., Tsai, L., Ingenito, E.P., Arold, S.P., Lutchen, K.R. and Suki, B. (2006) Comparison of variable and conventional ventilation in a sheep saline lavage lung injury model. *Critical Care Medicine*, **34**, 439-445. http://dx.doi.org/10.1097/01.CCM.0000196208.01682.87

[12] Thammanomai, A., Hueser, L.E., Majumdar, A., Bartolak-Suki, E. and Suki, B. (2008) Design of a new variable-ventilation method optimized for lung recruitment in mice. *Journal of Applied Physiology*, **104**, 1329-1340. http://dx.doi.org/10.1152/japplphysiol.01002.2007

[13] Spieth, P.M., Carvalho, A.R., Pelosi, P., Hoehn, C., Meissner C., Kasper, M., Hubler, M., von Neindorff, M., Dassow, C., Barrenschee, M., Uhlig, S., Koch, T. and de Abreu, M.G. (2009) Variable tidal volumes improve lung protective ventilation strategies in experimental lung injury. *American Journal of Respiratory and Critical Care Medicine*, **179**, 684-693. http://dx.doi.org/10.1164/rccm.200806-975OC

[14] Suki, B., Alencar, A.M., Sujeer, M.K., Lutchen, K.R., Collins, J.J., Andrade Jr., J.S., Ingenito, E.P., Zapperi, S. and Stanley, H.E. (1998) Life-support system benefits from noise. *Nature*, **393**, 127-128. http://dx.doi.org/10.1038/30127

[15] Wirtz, H.R. and Dobbs, L.G. (1990) Calcium mobilization and exocytosis after one mechanical stretch of lung epithelial cells. *Science*, **250**, 1266-1269. http://dx.doi.org/10.1126/science.2173861

[16] Arold, S.P. (2006) Effects of cyclic stretch on surfactant secretion and cell viability in alveolar epithelial cells grown in culture Diss. ProQuest, Boston University, UMI Dissertations Publishing, Boston.

[17] Venegas, J.G., Harris, R.S. and Simon, B.A. (1998) A comprehensive equation for the pulmonary pressure-volume curve. *Journal of Applied Physiology*, **84**, 389-395.

[18] Thammanomai, A., Majumdar, A., Bartolak-Suki, E. and

Suki, B. (2007) Effects of reduced tidal volume ventilation on pulmonary function in mice before and after acute lung injury. *Journal of Applied Physiology*, **103**, 1551-1559. http://dx.doi.org/10.1152/japplphysiol.00006.2007

[19] Hubmayr, R.D. (2002) Perspective on lung injury and recruitment: A skeptical look at the opening and collapse story. *American Journal of Respiratory and Critical Care Medicine*, **165**, 1647-1653. http://dx.doi.org/10.1164/rccm.2001080-01CP

[20] Thammanomai, A., Hamakawa, H., Bartolák-Suki, E. and Suki, B. (2013) Combined effects of ventilation mode and positive end-expiratory pressure on mechanics, gas exchange and the epithelium in mice with acute lung injury. *PLoS One*, **8**, Article ID: e53934. http://dx.doi.org/10.1371/journal.pone.0053934

[21] Wilson, T.A. and Bachofen, H. (1982) A model for mechanical structure of the alveolar duct. *Journal of Applied Physiology*, **52**, 1064-1070.

[22] Stamenovic, D. and Wilson, T.A. (1985) A strain energy function for lung parenchyma. *Journal of Biomechanical Engineering*, **107**, 81-86. http://dx.doi.org/10.1115/1.3138525

[23] Ingenito, E.P., Tsai, L.W., Majumdar, A. and Suki, B. (2005) On the role of surface tension in the pathophysiology of emphysema. *American Journal of Respiratory and Critical Care Medicine*, **171**, 300-304. http://dx.doi.org/10.1164/rccm.200406-770PP

[24] Denny, E. and Schroter, R.C. (1997) Relationships between alveolar size and fibre distribution in a mammalian lung alveolar duct model. *Journal of Biomechanical Engineering*, **119**, 289-297. http://dx.doi.org/10.1115/1.2796093

[25] Massa, C.B., Allen, G.B. and Bates, J.H. (2008) Modeling the dynamics of recruitment and derecruitment in mice with acute lung injury. *Journal of Applied Physiology*, **105**, 1813-1821. http://dx.doi.org/10.1152/japplphysiol.90806.2008

[26] Ingenito, E.P., Mark, L., Morris, J., Espinosa, F.F., Kamm, R.D. and Johnson, M. (1999) Biophysical characterization and modeling of lung surfactant components. *Journal of Applied Physiology*, **86**, 1702-1714.

[27] Ghadiali, S.N. and Gaver, D.P. (2008) Biomechanics of liquid-epithelium interactions in pulmonary airways. *Respiratory Physiology & Neurobiology*, **163**, 232-243. http://dx.doi.org/10.1016/j.resp.2008.04.008

[28] Amin, S.D., Majumdar, A., Frey, U. and Suki, B. (2009) Modeling the dynamics of airway constriction: Effects of agonist transport and binding. *Journal of Applied Physiology*, **109**, 553-563. http://dx.doi.org/10.1152/japplphysiol.01111.2009

[29] Wilson, T.A., Anafi, R.C. and Hubmayr, R.D. (2001) Mechanics of edematous lungs. *Journal of Applied Physiology*, **90**, 2088-2093.

[30] Vlahakis, N.E., Schroeder, M.A., Pagano, R.E. and Hubmayr, R.D. (2002) Role of deformation-induced lipid trafficking in the prevention of plasma membrane stress failure. *American Journal of Respiratory and Critical Care Medicine*, **166**, 1282-1289. http://dx.doi.org/10.1164/rccm.200203-207OC

